X-ray photoelectron and Auger-electron forward scattering: A new tool for studying epitaxial growth and core-level binding-energy shifts

W. F. Egelhoff, Jr.
*Surface Science Division, National Bureau of Standards,
Washington, D.C. 20234*

Above a few hundred eV kinetic energy, Auger electrons and photoelectrons exhibit strong forward scattering by overlying atoms, and this produces intensity peaks at polar and azimuthal angles corresponding to internuclear axes. This provides a new structural probe which is especially useful for studying epitaxy, surface alloying, and surface segregation. It also provides a new approach to measuring core-level binding-energy shifts by permitting selective enhancement of bulk versus surface signals.

A phenomenon generally referred to as electron channeling (or Kikuchi bands) has long been known in angular dependent x-ray photoelectron spectroscopy (XPS) of single crystals.[1] The phenomenon takes the form of enhanced XPS peak intensities along major crystal axes. Recent theoretical work suggests that the phenomenon might also be explained on the basis of a single-scattering model for photoelectrons.[2] [Experimentally it has been demonstrated that single scattering dominates the C_{1s} angular intensity dependence in CO on Ni(100).[3]] The present work demonstrates the single scattering, in particular, forward scattering, and not electron channeling (or Kikuchi bands) is the physical basis for the enhanced XPS peak intensities along major crystal axes of Cu(100), Ni(100), etc. The implication is that this explanation holds for XPS of other crystals as well. Moreover, this phenomenon is found to be a useful new tool for studies of surface structural and electronic properties. By enhancing the XPS peak intensities along the direction of internuclear axes, structural questions such as whether interdiffusion occurs when one metal is deposited on the surface of another or whether a deposited film lies flat or agglomerates into clusters can be readily and easily answered. This phenomenon also provides a new method for separating the surface and bulk components of the spectra because it allows the intensities of the surface and bulk components to be varied independently. The advantage of this is that it avoids previously required assumptions about line shapes or other deconvolution parameters.

In this work a number of epitaxial metal films have been investigated. They include Mn, Fe, Co, Ni, and Cu on Ni(100) and Cu(100) as well as sandwich structures with alternating layers of these. The most thoroughly studied system is Cu on Ni(100), and it provides results typical of the layer-by-layer growth mode.[4] Examples of these results are presented in Figs. 1(a) and 1(b) and consist of plots of the spectral peak intensities versus polar angle. Figures 1(a) and 1(b) demonstrate the evolution in shape of these polar intensity plots (PIP's) with Cu overlayer thickness. For 1 ML (monolayer) or less of Cu, the Cu $2p_{3/2}$ core level exhibits a featureless intensity variation (resembling the instrument response) as a function of polar angle in the $\langle 100 \rangle$ surface azimuth. Between 1 and 2 ML a peak grows in at 45° which can be explained on the basis of enhanced forward scattering of $2p_{3/2}$ photoelectrons from the first Cu layer [see Fig. 1(c)] by Cu atoms in the second layer. This is quite reasonable since recent work has shown that at kinetic energies above a few hundred eV, photoelectrons exhibit pronounced enhancement in their intensities along axes toward neighboring atoms due to constructive interference in this direction between the initial and scattered outgoing waves.[5]

It was consistently found in this work that more detail is observed in the PIP's for electron kinetic energies larger than the 317 eV of Fig. 1(a) (e.g., by studying shallower core levels). Figure 1(b) is such a case, being the x-ray-induced Cu $2p3d3d$ Auger peak (Auger electrons should exhibit the same scattering properties as x-ray photoelectrons[6]) intensity versus polar angle. Here, two peaks are resolved for 2-ML Cu, at 45° and $\sim 70°$, corresponding again to Fig. 1(c). At larger Cu thicknesses peaks grow in at 0° and 20° due to forward scattering involving deeper Cu atoms. Results on the Cu $3p$ ($E_k = 1173$ eV) and Cu $3d$ ($E_k = 1246$ eV) peaks for Cu on Ni(100) are very similar to those of Fig. 1(b), indicating that above a few hundred eV all Auger and photoelectrons give similar results. Moreover, the PIP's for the Ni peaks of clean Ni(100) are very similar to the Cu peaks of the 14-ML Cu case of Figs. 1(a) and 1(b) [14 ML is thick enough to be essentially converged (to $\sim 98\%$) of the results for bulk Cu(100)].

It is important to note (and this has been confirmed by studying sandwich films, e.g. Cu/Ni/Cu, Ni/Fe/Ni, Cu/Mn/Cu, Cu/Co/Cu, Cu/Fe/Cu, etc.) that since atoms like Co, Ni, and Cu have very similar scattering properties, the contribution each atom makes to a PIP plot depends only on the layer it is in and not on the identity of the surrounding atoms. Thus, in Figs. 1(a) and 1(b) the intensity contribution from the top Cu layer in a multilayer Cu film will equal that from 1 ML of Cu on Ni(100). This allows the surface layer contribution as a percent of the total to be determined, as shown in Fig. 1(d). Here, the 1-ML intensity is divided by the total intensity, thus accurately quantifying for the first time the top 1-ML contribution to the Cu $2p_{3/2}$ and CVV peaks in bulk Cu(100).

It can be readily seen in Figs. 1(a) and 1(b) that electron channeling (the Kikuchi effect) is not responsible for the peaks in the PIP's. Channeling, for example, along $\langle 110 \rangle$ planes of Cu, i.e., the 45° peak in Fig. 1(b), could not even begin until a Cu thickness of ~ 12 ML [to satisfy the first-order Bragg condition for $E_k \approx 1000$ eV and a $\sim 10°$ full-width at half maximum (FWHM) PIP peak; see Ref. 2]. The situation is even worse for the other PIP peaks in Figs. 1(a) and 1(b). However, the peaks in the PIP's are fully developed for very thin Cu layers, e.g., 2 ML for the 45° peak in Figs. 1(a) and 1(b). Deeper layers tend to make a

EPITAXIAL Cu ON Ni(100)

INTENSITY (KCPS)

$E_k = 317$ eV

(a)

Cu $2p_{3/2}$

MLCu

14
3.3
2.1
0.94

80 60 40 20 0

CuCVV AUGER
$E_k = 917$ eV

(b)

14
3.3
2.1
0.94

80 60 40 20 0

θ, DEGREES OFF SURFACE NORMAL

Ni(100) XPS Ni $2p_{3/2}$

(f)

45°   55°

TOTAL
BULK
SURFACE

TOTAL
BULK
SURFACE

858 856 854 852 E_B (eV) 858 856 854 852

EFFECTS OF ADSORBED GASES ON SURFACE Ni

(g)

• CLEAN FROM (f) ABOVE, (X2)

• WITH c(2X2)-OXYGEN

• c(2X2)-CO "ON TOP" 0.5ML Ni

• REMAINING "CLEAN" Ni ATOMS (0.5ML)

858 856 854 852 E_B (eV) 858 856 854 852

ANGLES FOR ENHANCED FORWARD SCATTERING

<100> CRYSTAL AXES

<100>

(c)

45°   71.6°

2 ML Cu

ON Ni(100)

AT 45°

Ni $2p_{3/2}$

(h)

ADD 1.5ML Cu

0.3ML Ni

ON Cu(100)

855   850 E_B (eV)

Ni(100) XPS Ni $2p_{3/2}$ ATTENUATION BY OVERLAYERS

(i)

EXPECTED

ACTUAL AT 45°

INTENSITY (ARB. UNITS)

1 2 3

Cu THICKNESS (ML)

INTENSITY FROM SURFACE LAYER AS A % OF THE TOTAL FROM Cu(100)

%

(d)

60

40

20

0

$2p_{3/2}$

CVV AUGER

80 60 40 θ 20 0

(e)

← 932.28eV

← 932.46eV
← 932.57eV

← 932.52eV
← 932.63eV
← ~932.60eV

← 932.56eV

932.70eV

Ni(100) XPS Mgkα

(j)

2p

EXHIBITS ENHANCEMENT AT 45°

CVV AUGER

EXHIBITS NO ENHANCEMENT

3p

3s

3d

INTENSITY
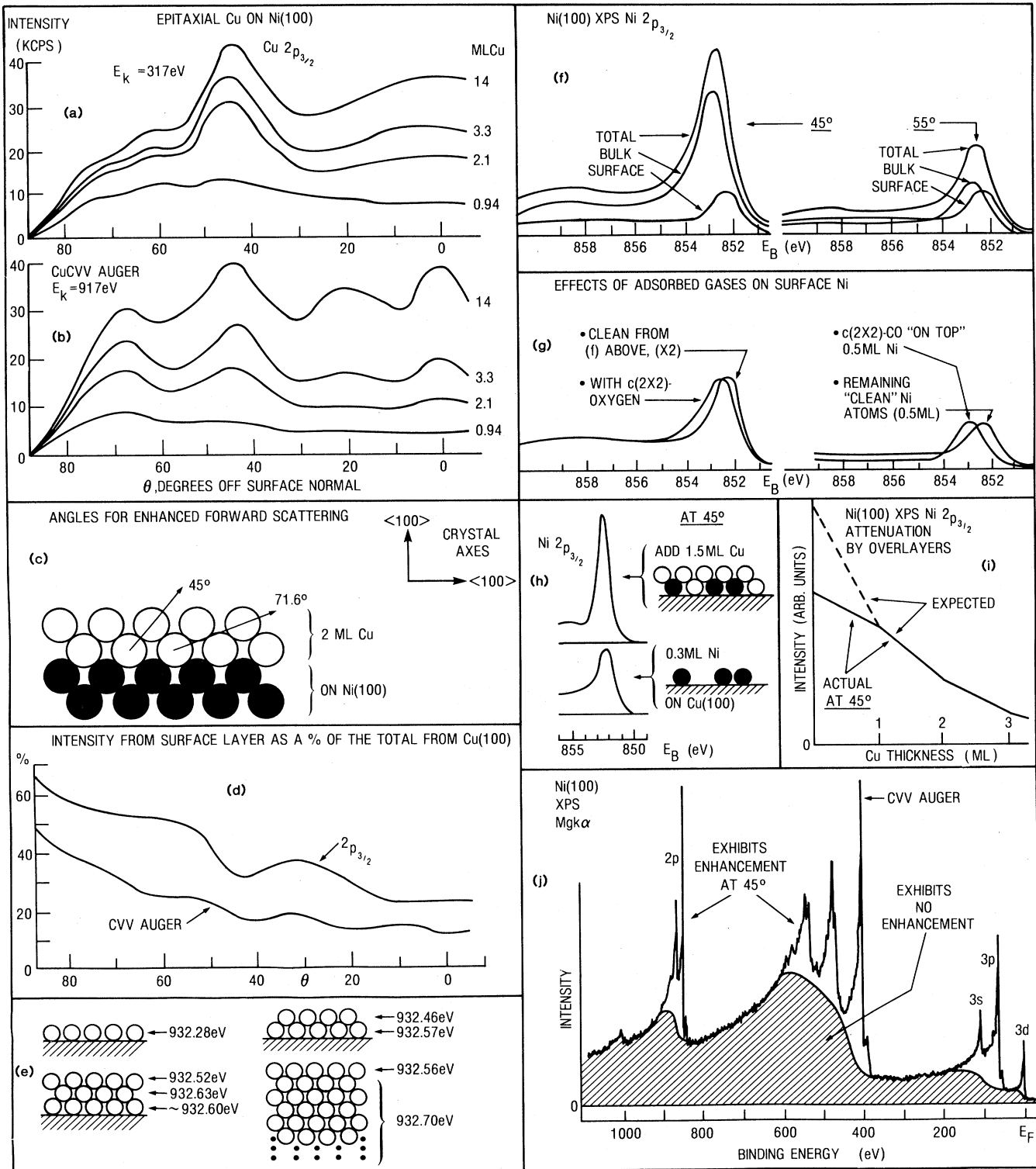
1000 800 600 400 200 E_F

BINDING ENERGY (eV)

FIG. 1. Intensity vs polar angle of (a) the Cu $2p_{3/2}$ and (b) the Cu CVV Auger peaks for epitaxial Cu on Ni(100) as a function of Cu thickness in monolayers (ML); (c) an illustration of angles at which forward scattering of electrons from the bottom Cu layer by the top Cu layer causes enhanced Cu intensities for 2-ML Cu on Ni(100); (d) the Cu $2p_{3/2}$ and CVV Auger contribution of the surface Cu layer as a percent of the total from bulk Cu(100); (e) the Cu $2p_{3/2}$ binding energies for Cu layers of various thicknesses, the shaded substrate being Ni(100); (f) the separation of the Ni $2p_{3/2}$ spectrum into its components; (g) the effect of adsorbed O and CO on the surface Ni $2p_{3/2}$ peak; (h) the sharp increase at 45° in Ni $2p_{3/2}$ intensity upon encasing Ni in Cu; (i) the actual attenuation of Ni $2p_{3/2}$ by Cu overlayers and that expected if the attenuation above 1 ML were extrapolated (see text) from 1 ML to zero; and (j) the breakdown of the entire spectrum into parts enhanced and not enhanced at 45°.

smooth contribution to the PIP's as can be seen in the difference between the 14- and 3.3-ML PIP's. Thus, forward scattering by relatively nearby overlying atoms[5] is predominantly responsible for the peaks in the PIP's.

In studies of clean Ni(100), smearing out of the Ni PIP peaks is observed at elevated temperatures (e.g., from 100 to 1000 K) and is consistent with rms atomic displacements broadening the forward-scattering cones. If the PIP peaks were due to diffraction off the lattice, the Debye-Waller effect would predict much larger reductions in PIP peak intensities at elevated temperatures than are observed. (The Debye-Waller factor is zero for forward scattering.) This supports the forward-scattering interpretation.

This understanding of the origin of peaks in PIP's can readily be used as a new tool in studying core-level binding-energy shifts. For example, from Fig. 1(a) it is clear that in going from 55° to 45° in the 14-ML PIP there is a big increase in the $2p_{3/2}$ signal from the deeper Cu layers but almost no change in the surface Cu layer [as evidenced by the 0.94-ML spectrum in Fig. 1(a)]. Thus, the Cu $2p_{3/2}$ difference spectrum 45°–55° gives the bulk spectrum for Cu.[7] The percentage of the total spectrum due to the surface (with the balance due to the bulk) is known [Fig. 1(d)]. Knowing the percentage of the total due to the bulk allows the bulk spectrum (45°–55°) to be scaled to the correct size [using Fig. 1(d)] and subtracted from the total spectrum to leave only the surface spectrum. This approach enables the separation of the core-level binding energies for a variety of epitaxial layer cases. Examples of such results are presented in Fig. 1(e) for the Cu $2p_{3/2}$ level of Cu layers on Ni(100). This approach to separating core-level peaks has the advantage of avoiding assumptions previously required about line shapes and deconvolution parameters.[8,9]

An example of such a separation of contributions in core-level spectra is presented in Fig. 1(f) for the $2p_{3/2}$ peak of clean Ni(100). The surface core-level shift (SCLS) in Fig. 1(f) is 0.43 eV. This value provides a check on the accuracy of this method of measuring SCLS's since a different approach yielded 0.46 eV for this quantity,[9] signifying good agreement.[10] For a clear understanding of Fig. 1(f), note that the illustrated bulk spectrum is just the difference spectrum 45°–55° with its height scaled according to the percentage of the total spectrum coming from the bulk [determined as for Cu in Fig. 1(c)].

This approach also makes it easier to extract the core-level shifts for surface metal atoms which occur upon adsorption of gases. Figure 1(g) shows the clean Ni(100) surface $2p_{3/2}$ peak [×2 relative to Fig. 1(f)] and the Ni(100) surface $2p_{3/2}$ peak (also ×2) with a $c(2\times2)$-oxygen overlayer, exhibiting a peak shift of 0.25 eV. Also illustrated in Fig. 1(g) is the Ni $2p_{3/2}$ surface peak shift induced by CO adsorbed in a $c(2\times2)$-CO structure. Since this structure consists of half the surface Ni atoms with CO adsorbed in the on-top position and half of the surface Ni atoms "clean,"[11] the total surface Ni intensity is separated into the two illustrated components assuming the "clean" Ni atoms exhibit the same peak position as in Fig. 1(f). This separation produces a shift of 0.67 eV. Such shifts are very important when used with the equivalent-core-approximation interpretative framework (see Ref. 9 for details) in which the CO-induced Ni $2p_{3/2}$ shift should correspond to the difference in the heat of CO adsorption on Ni and Cu. For

Ni(100) and Cu(100) those heats differ by 0.72 eV,[12] in remarkably good agreement.

Figure 1(f) demonstrates the dramatic increase which occurs in the bulk signal intensity in going from 55° to 45° due to forward scattering. One way this dramatic effect may be observed without any data manipulation is presented in Fig. 1(h), which demonstrates the sharp increase that occurs in the Ni $2p_{3/2}$ peak at 45° when 0.3-ML Ni on Cu(100) is covered by 1.5 ML of Cu. (At 55°, in contrast, a decrease is observed.) This is the first example known in which an overlayer can increase the substrate XPS signal intensity rather than attenuate it. Many other examples of this have been found in the present work using other combinations of metal layers; however, Fig. 1(h) is the most dramatic.

Figure 1(i) shows another of the many manifestations of the enhanced forward-scattering phenomenon. When Cu is deposited layer by layer on Ni(100) the Ni $2p_{3/2}$ intensity would normally be expected to fall in a series of straight line segments with each added complete Cu monolayer, producing the same percentage drop (an exponential) in the Ni $2p_{3/2}$ signal. At 45° this is quite true above 1-ML Cu but from zero to 1 ML the drop, as seen in Fig. 1(i), is much less than would be expected on the basis of the actual magnitude of the subsequent drops for thicker Cu overlayers in Fig. 1(i). The reason is clearly that the first Cu layer enhances the Ni $2p_{3/2}$ intensity of the top Ni layer, partially offsetting the drop due to the expected attenuation.

One obvious benefit provided by the above examples is a much clearer understanding of some of the limitations and complexities inherent in the notions of electron inelastic mean free paths or escape depths which are so widely used in XPS and Auger spectroscopy.

One last example of the relevance of this phenomenon is presented in Fig. 1(j). In broad scans of the entire spectrum it was found that the large background of inelastic secondary electrons showed no enhancement (e.g., 45°–55°). The unshaded areas in Fig. 1(j) have exactly the shape of the difference spectrum 45°–55°. The shaded areas of Fig. 1(j) represent what is left behind when the 45°–55° difference spectrum is used to strip away entirely the elastic peaks. Thus, a separation is obtained in which the shaded areas correspond to the isotropic inelastic background and the unshaded areas correspond to intrinsic elastic (main peaks) and intrinsic inelastic (shakeup) emission together with a small contribution,[13] due to forward-scattered extrinsic inelastic emission (i.e., initially intrinsic emission with energy loss on the way out). Such results help provide a better understanding of the breakdown of the spectrum into its constituent parts.

In conclusion, it should be emphasized that enhanced forward scattering is a new tool for surface structural and electronic properties that can readily be applied to a wide range of metal, semiconductor, insulator, and alloy systems. For example, at present, relative quick (~10 s) PIP scans are being found very useful in real-time studies of surface segregation, interdiffusion, and surface alloying in various combinations of Cu on Ni and Ni on Cu. Furthermore, it should be noted that a large increase in PIP sensitivity (an order of magnitude) would be possible using electron-induced Auger rather than the x-ray-induced Auger studies reported here.

[1]K. Siegbahn, U. Gelius, H. Siegbahn, and E. Olson, Phys. Lett. **32A**, 221 (1970); C. S. Fadley and S. Å. L. Berström, *ibid.* **35A**, 375 (1971); N. E. Erickson, Phys. Scr. **16**, 462 (1977).

[2]S. M. Goldberg, R. J. Baird, S. Kono, N. F. T. Hall, and C. S. Fadley, J. Electron. Spectrosc. Relat. Phenom. **21**, 1 (1980).

[3]L.-G. Peterson, S. Kono, N. F. T. Hall, C. S. Fadley, and J. B. Pendry, Phys. Rev. Lett. **42**, 1545 (1979).

[4]The experimental details for this work are presented in W. F. Egelhoff, Jr., J. Vac. Sci. Technol., A **2**, 350 (1984).

[5]S. Kono, C. S. Fadley, N. F. T. Hall, and Z. Hussain, Phys. Rev. Lett. **41**, 117 (1978); see especially Fig. 3 in S. Kono, C. S. Fadley, N. F. T. Hall, and Z. Hussain, Phys. Rev. B **22**, 6085 (1980).

[6]C. S. Fadley, in *Progress in Surface Science,* edited by S. G. David-son (Pergamon, New York, in press).

[7]Note, the assumption is made here that the second and deeper layers have the same core-level binding energy. This is almost certainly true within the experimental uncertainty of ± 0.04 eV.

[8]For a typical deconvolution, see D. E. Eastman, T.-C. Chiang, P. Heiman, and F. J. Himpsel, Phys. Rev. Lett. **45**, 656 (1980).

[9]W. F. Egelhoff, Jr., Phys. Rev. Lett. **50**, 587 (1983).

[10]The estimated uncertainty in SCLS determinations is ± 0.04 eV.

[11]J. P. Biberian and M. A. Van Hove, Surf. Sci. **118**, 443 (1982).

[12]J. C. Tracy, J. Chem. Phys. **56**, 2736 (1972); **56**, 2748 (1972).

[13]For example, electron-energy-loss spectra in this energy range from Ni show the intensity of the inelastic tail is less than 5% of the elastic peak at a loss of 10 eV. C. J. Powell (unpublished).